

THERMODYNAMICS OF INORGANIC COMPOUNDS

Thermodynamic Properties of Europium-Doped BaLa₂WO₇-Based Compounds

D. B. Gogol^a, D. T. Sadyrbekov^{a, b}, and M. R. Bissengaliyeva^{a, *, **}

^aInstitute of Problems of Complex Development of Mineral Resources, Karaganda, 100019 Republic of Kazakhstan

^bBuketov Karaganda State University, Karaganda, 100028 Republic of Kazakhstan

*e-mail: 160655@mail.ru

**e-mail: mirabis@ipkon.kz

Received November 15, 2019; revised December 2, 2019; accepted December 24, 2019

Abstract—Samples of compounds were synthesized by the solid-phase method from the systems of barium, lanthanum, europium, and tungsten ternary oxides with the general formula Ba(La, Eu)₂WO₇. The unit cell parameters were refined, and the content of additional phases was determined using the full-profile calculation of X-ray diffraction patterns. The heat capacities of these samples were studied by adiabatic calorimetry from the helium region to room temperatures (4.25–315 K), and the anomalies produced by the doping element were detected. Based on the experimental data, the lattice component of the heat capacity was recognized to determine the entropy and enthalpy changes in the anomalies, and the thermodynamic functions of the compounds were calculated within a range of 5–310 K. The standard thermodynamic functions are $C_{p,298.15} = 208.3 \pm 0.7$ J/(mol K), $S_{298.15}^{\circ} = 243.6 \pm 1.5$ J/(mol K), and $H_{298.15} - H_0 = 37360 \pm 185$ J/mol for Ba(La_{0.99}Eu_{0.01})₂WO₇, $C_{p,298.15} = 208.7 \pm 0.5$ J/(mol K), $S_{298.15}^{\circ} = 244.0 \pm 1.2$ J/(mol K), and $H_{298.15} - H_0 = 37619 \pm 142$ J/mol for Ba(La_{0.97}Eu_{0.03})₂WO₇, and $C_{p,298.15} = 208.8 \pm 0.8$ J/(mol K), $S_{298.15}^{\circ} = 242.6 \pm 1.5$ J/(mol K), and $H_{298.15} - H_0 = 37384 \pm 190$ J/mol for Ba(La_{0.95}Eu_{0.05})₂WO₇.

Keywords: ternary oxides, rare-earth elements, lanthanum, low-temperature heat capacity, adiabatic calorimetry

DOI: 10.1134/S0036023620050101

INTRODUCTION

The compounds and materials based on rare-earth elements (REEs) with different properties are widespread and highly demanded in contemporary technology. Among the REE compounds with a pyrochlore-related structure there are ferroelectrics, magnetics, semiconductors, and superconductors. The doping of compounds from the systems of complex oxides with REE atoms appreciably expands the spectrum of their promising properties. Due to the specific features of the electronic structure of lanthanides, the synthesized compounds exhibit luminescent, dielectric, transport, and other properties. In view of a great variety of specific features and a considerable number of doping variants for these compounds, their physicochemical properties require systematic studies.

Among the dopants, a prominent place is held by europium, which has a high fluorescence period enabling its application in diverse materials [1]. For example, europium–tungstate systems are distinguished by an efficient transfer of energy between the WO₄²⁻ group and the Eu³⁺ ion, which enables their

application as luminescent light sources [2]. The samples of CaMoO₄:xEu³⁺ luminophors ($x = 1–6$ mol %) prepared by the sol-gel method, according to the reflection measurement results [3], are optically active compounds. Tungstate BaLa_{3.96}Eu_{0.04}(WO₄)₇ demonstrates red luminescence of medium efficiency at room temperature and lower and in the ultraviolet region [4].

Rather efficient luminophors are BaLa₂WO₇ based compounds, which show optical activity not only in the case of europium, but also with the other lanthanides [5–9]. Here, the possibilities of exhibiting the luminescent properties become broader with the combined application of two lanthanides or the partial substitution of the rare-earth element.

The number of works describing the thermodynamic properties of the europium doped compounds is much lower. Thus, the high-temperature heat capacity of (U_{1-x}Eu_x)O₂ compounds was studied within a temperature range from 300 to 1550 K in the work [10]. Hence, there is a gap in the study of the thermodynamic and other properties of these com-

Table 1. Parameters of the crystal structure of samples

Compound	Unit cell parameters, Å, deg				Unreliability factors, %	
	<i>a</i>	<i>b</i>	<i>c</i>	γ	R_p	R_{wp}
Ba(La _{0.99} Eu _{0.01}) ₂ WO ₇	8.8577	12.8804	5.8371	105.128	11.25	17.17
Ba(La _{0.97} Eu _{0.03}) ₂ WO ₇	8.8577	12.8769	5.8346	105.126	11.63	17.34
Ba(La _{0.95} Eu _{0.05}) ₂ WO ₇	8.8577	12.8752	5.8305	105.124	12.49	16.29

Atom	Ba(La _{0.99} Eu _{0.01}) ₂ WO ₇			Ba(La _{0.97} Eu _{0.03}) ₂ WO ₇			Ba(La _{0.95} Eu _{0.05}) ₂ WO ₇		
	<i>x</i>	<i>y</i>	<i>z</i>	<i>x</i>	<i>y</i>	<i>z</i>	<i>x</i>	<i>y</i>	<i>z</i>
Ba	0.4790	0.1267	0.5149	0.4826	0.1283	0.5099	0.4811	0.1339	0.5037
La/Eu(1)	0.1860	0.0929	0.0062	0.1883	0.0789	0.0023	0.1883	0.0913	0.9753
La/Eu(2)	0.0780	-0.1241	0.4717	0.0577	-0.1257	0.5025	0.0577	-0.1257	0.5025
W	0.2811	0.3378	0.4608	0.2920	0.3375	0.4690	0.2920	0.3444	0.4647
O(1)	0.4884	0.3361	0.4929	0.5087	0.3476	0.4620	0.4907	0.3476	0.4755
O(2)	0.0488	0.3140	0.4460	0.0511	0.3280	0.4769	0.0511	0.3232	0.4769
O(3)	0.2793	0.4423	0.7481	0.2996	0.4283	0.7173	0.2958	0.4407	0.7173
O(4)	0.2658	0.2458	0.1781	0.2455	0.2474	0.2090	0.2635	0.2474	0.1816
O(5)	0.3275	0.4688	0.2429	0.3072	0.4672	0.2463	0.3252	0.4548	0.2463
O(6)	0.2493	0.2002	0.6711	0.2470	0.2018	0.6402	0.2470	0.2142	0.6402
O(7)	-0.0009	-0.0026	0.2482	0.0014	0.0110	0.2791	0.0194	0.0114	0.2517

pounds at low temperatures, and this gap may be filled by the method of adiabatic calorimetry.

In the present work, the doped compounds with the general formula Ba(La_{1-x}Eu_x)₂WO₇, where *x* is the stoichiometric index depending on the taken molar ratios, were synthesized and measured. The molar ratios selected for the synthesis of these compounds corresponded to 1, 3, and 5 mol % of oxide Eu₂O₃ with respect to the number of lanthanum oxide La₂O₃ moles.

EXPERIMENTAL

The initial compounds used for synthesis were strontium carbonate SrCO₃, barium carbonate BaCO₃, tungsten(VI) oxide WO₃, lanthanum oxide La₂O₃, and europium oxide Eu₂O₃. The reagents were of chemically pure (REE oxides), pure (barium and strontium carbonates), and pure for analysis (tungsten oxide) grades. Oxides of alkali-earth and rare-earth metals were additionally calcined before synthesis at 1173 K (900°C) for 2 h to remove the excessive water and adsorbed carbon dioxide. Complex oxides were synthesized by the solid-phase method. The precisely weighed portions of the initial reagents taken in stoichiometric amounts were carefully ground in an agate mortar, and the resulting mixture was further annealed at a temperature of 973 K (700°C) for 10–12 h in porcelain crucibles in an air atmosphere. Afterwards, the prepared precursors were triturated in an agate mortar and calcined in aluminum crucibles in an air atmosphere at a sequential increase in temperature from 1173 K (900°C, 6 h) to 1273 K (1000°C, 6 h) with triple terminal annealing at 1473 K (1200°C) for 7 h.

The X-ray diffraction patterns of the synthesized samples were recorded on a Shimadzu XRD-6000 diffractometer at room temperature (CuK α radiation; reflection geometry; range of angles $2\theta = 10^\circ\text{--}60^\circ$; step, 0.02°). The processing of recorded X-ray diffraction patterns, the detection of known phases, and the search for isostructural compounds were performed by the Match! Version 2.3 software [11] and the PDF-2 powder X-ray diffraction database [12]. The primary indexing of X-ray diffraction patterns and the determination of the symmetry system, space groups, and unit cell parameters of the compounds were performed by the DicVol06, Treor-90, and ITO programs incorporated into the FullProf software suite [13]. The modeling of difference X-ray diffraction patterns and the refinement of unit cell parameters on the basis of data for the selected isostructural compounds were performed in the Powder Cell Version 2.4 software [14]. Crystal structure parameters were determined by means of sequential refinement first for general X-ray diffraction pattern parameters and then for unit cell parameters and peak shapes with further optimization of atomic positions.

The heat capacity of the samples was measured from the liquid helium temperature by adiabatic calorimetry on a Termax low-temperature thermophysical setup [15]. The portions of the samples were from 1.3 to 2.2 g in weight. The titanium containers with samples were evacuated, filled with gaseous helium, and sealed with an indium gasket. The step of measurements was varied from 0.3 to 3 K depending on the temperature range, and the region of measurements was 4.25–320 K. The common temperature range of measurements was passed several times, and in the

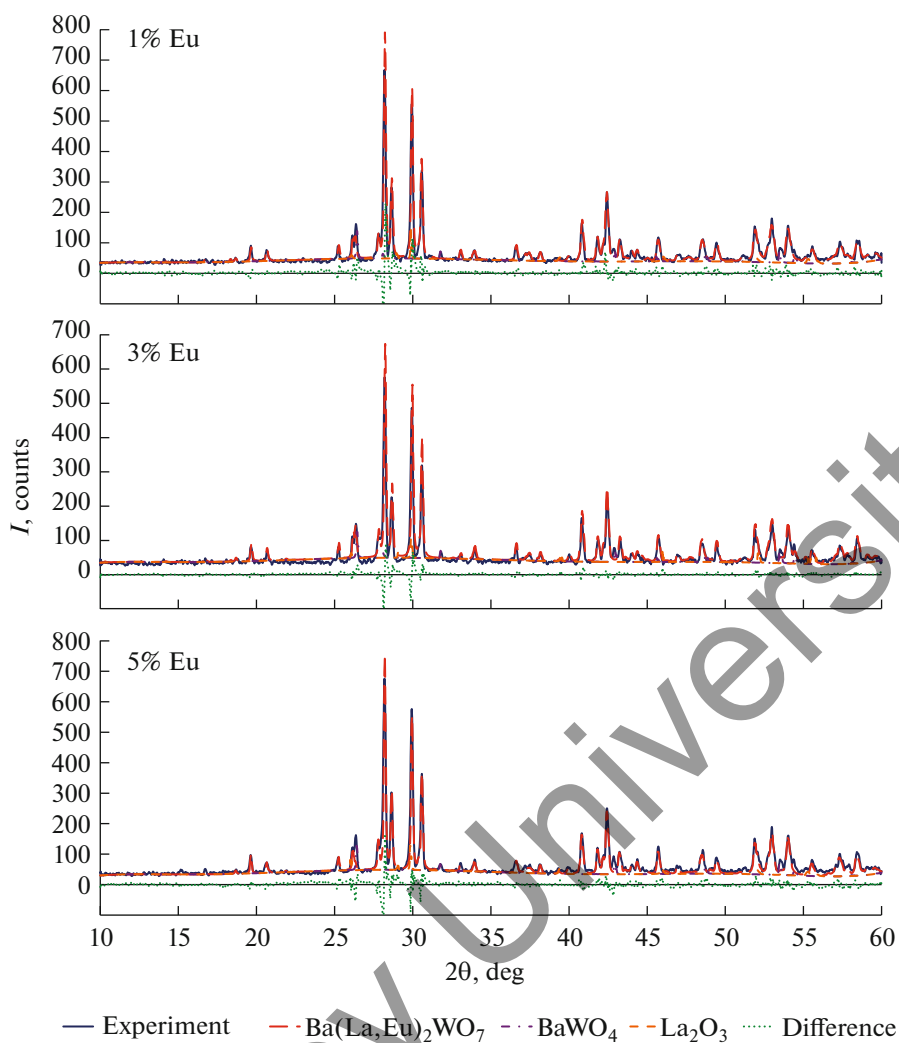


Fig. 1. Experimental, theoretical, and difference X-ray diffraction patterns of $\text{Ba}(\text{La}_{1-x}\text{Eu}_x)_2\text{WO}_7$.

region of temperatures below 20 K, heat capacity measurements were performed no less than three times.

The measured data were processed via the spline approximation of experimental heat capacity values with cubic polynomials like $C_p = a_0 + a_1T + a_2T^2 + a_3T^3$. Below the temperature of 5 K, heat capacity values were extrapolated to absolute zero in compliance with the odd-degree polynomial $C_p = aT^3 + bT^5$. Overlapping in the region of changing the polynomials was no less than 3–4 experimental points

RESULTS AND DISCUSSION

The X-ray diffraction analysis of the samples showed good correspondence to BaLa_2WO_7 (PDF-2, no. 00-039-0083) [16, 17], which crystallizes in monoclinic system (space group $P112_1/b$). In addition to the major phase, all samples were found to contain trace amounts of incompletely converted initial compounds

presented by barium tungstate BaWO_4 (PDF-2, no. 00-008-0457) and lanthanum oxide La_2O_3 (PDF-2, no. 01-076-7398), whose content was estimated as ~3–4 vol %. The impurities were present at nearly equal molar ratios, which argues for the absence of non-stoichiometry in the target compounds. No any other impurities have been detected.

The results of crystal structure refinement for the synthesized compounds with consideration for the partial occupancies of lanthanum atomic positions by europium atoms are given in Table 1. The crystallographic positions of atoms in a unit cell of the samples correspond to the atomic positions from the paper [17] with a deviation of no more than $\pm 2\%$.

As can be seen from the obtained data, the linear unit cell parameters b and c are slightly decreased with increasing europium content in the samples, whereas the monoclinic angle remains almost unchanged. This circumstance is explained by that the ionic radius of europium is rather close to the values for lanthanum

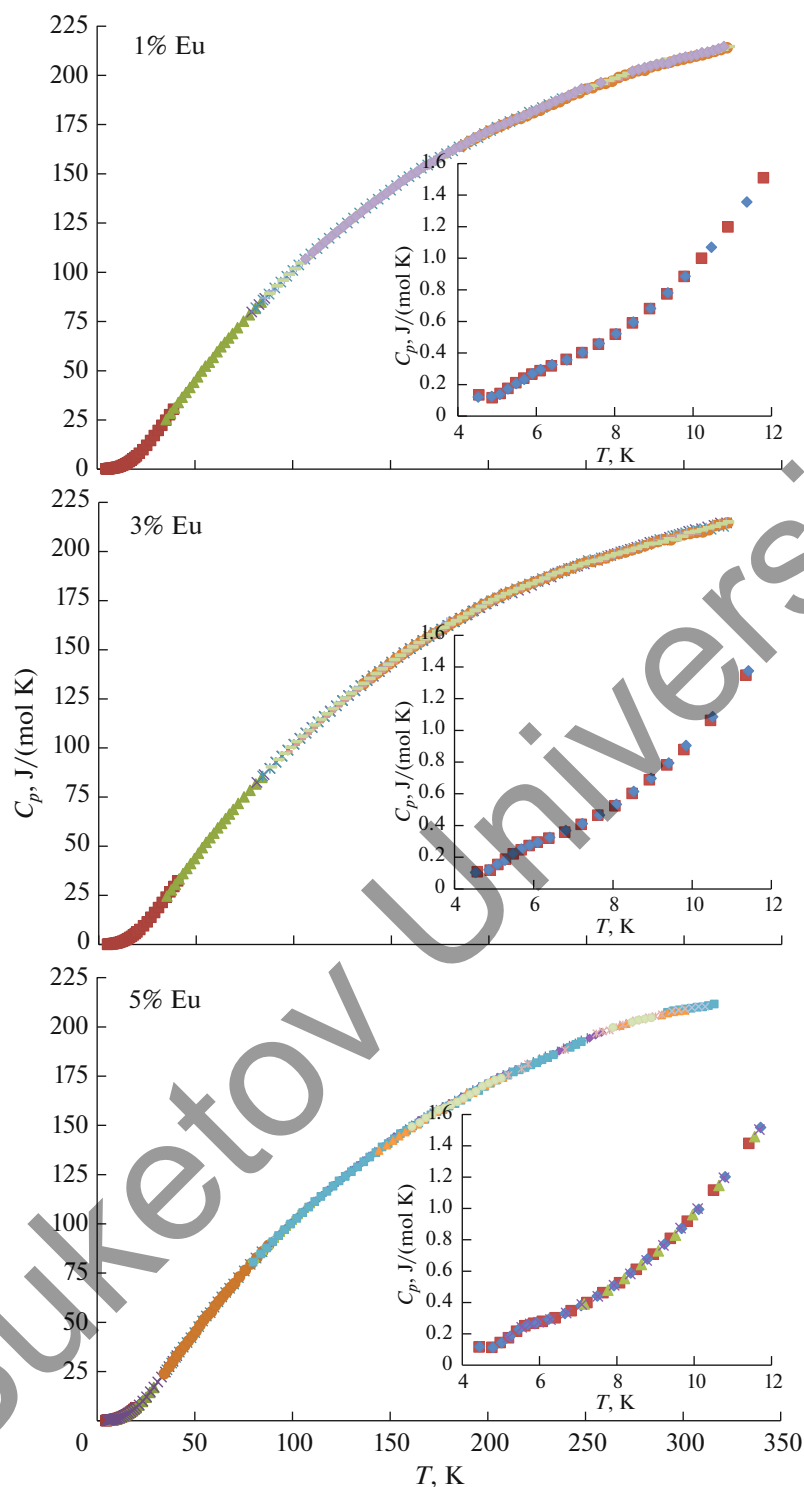


Fig. 2. Experimental molar heat capacity of the studied $\text{Ba}(\text{La}_{1-x}\text{Eu}_x)_2\text{WO}_7$.

atoms, and the unit cell parameters of the compounds are only slightly changed.

The experimental, theoretical, and difference X-ray diffraction patterns of the compounds are shown in Fig. 1. The difference curves were obtained by subtracting the sum of theoretical profiles of the

doped major compound and impurities, which are also taken into account in calculation, from the experimental X-ray diffraction pattern.

The refined content of barium tungstate and lanthanum oxide impurities in the samples on molar basis is 7.3 mol % for the sample with 1% of Eu, 6.8 mol %

for the sample with 3% of Eu, and 7.8 mol % for the sample with 5% of Eu each. From this data it follows that the major phase content in the samples is 92.13, 92.72, and 91.71 wt %, respectively.

Taken into account the BaWO₄ and La₂O₃ impurities found in the samples, the correction for their content was applied to the experimental heat capacity data. The specific heat capacities of barium tungstate [18] and lanthanum oxide [19] was subtracted from the total experimentally measured heat capacity in proportion to the weight content of an impurity.

The heat capacity–temperature dependences obtained as a result of the calorimetric measurements are shown in Fig. 2. The low-temperature heat capacity of the samples was shown to have abnormal deviations from the conventional heat capacity behavior due to the presence of Eu³⁺ ions in their crystal structure. The anomalies look like gentle low-intensity peaks within a range from 5 to 8 K.

The abnormal component of the heat capacity was calculated via the transformation and subtraction of the lattice component from the total heat capacity according to the equations [20, 21]

$$\frac{C_L}{T^3} = K \left(1 - \frac{C_L}{3Rn} \right)^m, t$$

$$\ln \left(\frac{C_L}{T^3} \right) = m \ln \left(1 - \frac{C_L}{3Rn} \right) + \ln K.$$

The smoothed dependences shown in Fig. 3 were obtained for the isolated abnormal and lattice components of the heat capacity. The equations of these dependences were used to calculate the enthalpy and entropy changes in the observed abnormal transitions.

The heat capacity anomalies seem to appear due to the possible occurrence of magnetic interactions in the samples because of the presence of europium atoms. Natural europium generally consists of two isotopes, ¹⁵¹Eu and ¹⁵²Eu, which have a spin of 5/2 predetermining the existence of magnetic properties for its compounds. The found enthalpy and entropy changes in the anomalies of the samples only slightly vary despite an increase in europium content: from 0.19 to 0.26 J/mol and from 0.030 to 0.042 J/(mol K), respectively, in compliance with the error estimated at a level of ±15%. This circumstance may indicate that the observed effects do not directly depend on the doping element concentration. The values of entropy change in the observed transitions are much smaller than the theoretical value $R \ln 2$ due to that the lanthanum atoms are only partially substituted by europium atoms during the doping of these compounds. Being calculated per mole of europium atoms with consideration for its molar content in a compound, these parameters are 4.01–5.55 J/mol and 0.646–0.895 J/(mol K), respectively.

The major thermodynamic functions of the synthesized compounds, such as the entropy S° and the enthalpy change $H_T - H_0$, were determined from the coefficients of approximating polynomials as follows:

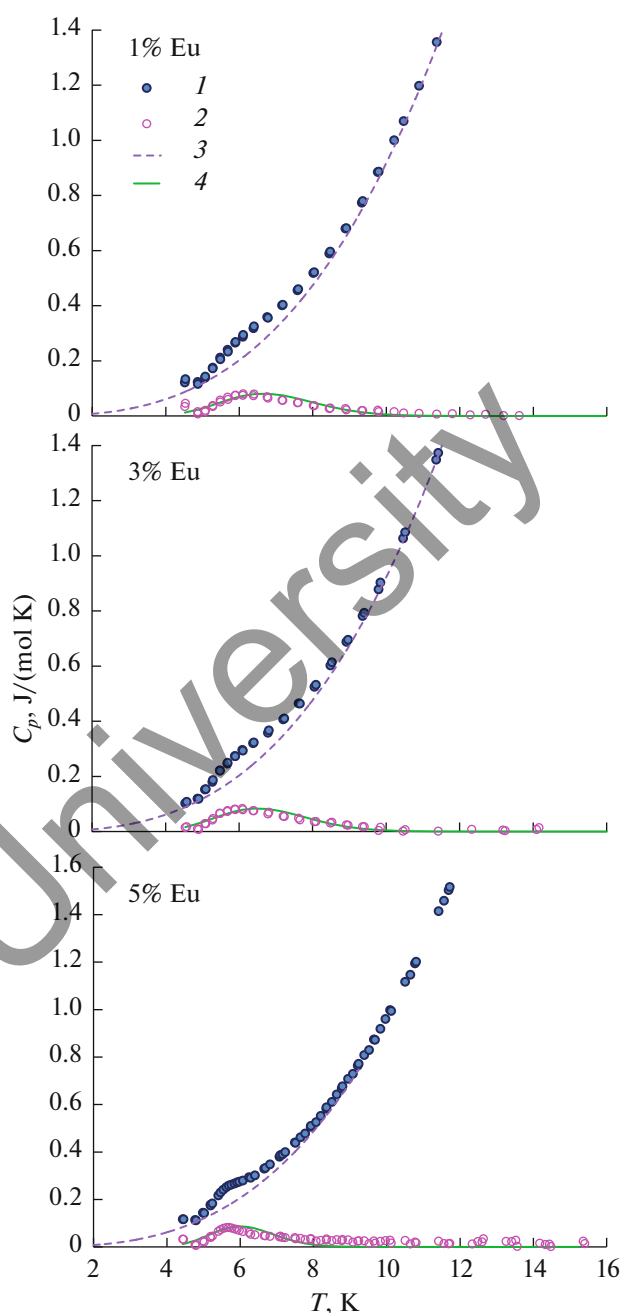


Fig. 3. (1) Total, (2) abnormal, (3) lattice, and (4) smoothed abnormal heat capacities of Ba(La_{1-x}Eu_x)₂WO₇.

$$S_T^\circ = \int_0^T \frac{C_p}{T} dT = a_0 \ln T + \sum_{n=1}^3 \frac{a_n T^n}{n},$$

$$H_T^\circ - H_0^\circ = \int_0^T C_p dT = \sum_{n=0}^3 \frac{a_n T^{n+1}}{n+1}.$$

The thermodynamic functions of the studied compounds calculated within the range 5–300 K are given in Table 2, together with corresponding errors. The measurement errors were determined from the spread

Table 2. Thermodynamic functions of compounds

<i>T</i> , K	Ba(La _{0.99} Eu _{0.01}) ₂ WO ₇			Ba(La _{0.97} Eu _{0.03}) ₂ WO ₇			Ba(La _{0.95} Eu _{0.05}) ₂ WO ₇		
	<i>C_p</i> , J/(mol K)	<i>S^o</i> , J/(mol K)	<i>H_T – H₀</i> , J/mol	<i>C_p</i> , J/(mol K)	<i>S^o</i> , J/(mol K)	<i>H_T – H₀</i> , J/mol	<i>C_p</i> , J/(mol K)	<i>S^o</i> , J/(mol K)	<i>H_T – H₀</i> , J/mol
5	0.134	0.029	0.119	0.137	0.026	0.108	0.143	0.027	0.113
10	0.939	0.333	2.523	0.938	0.333	2.529	0.966	0.335	2.549
20	6.601	2.368	35.04	6.634	2.379	35.24	6.685	2.417	35.79
30	17.99	7.023	153.7	17.90	7.046	154.1	18.17	7.119	155.7
40	34.82	14.70	424.2	31.48	14.06	401.1	31.64	14.20	405.1
50	51.44	24.23	854.3	45.05	22.54	783.9	44.99	22.70	788.3
60	57.81	33.58	1369	57.90	31.90	1299	57.85	32.04	1303
70	69.65	43.39	2007	69.91	41.74	1939	69.83	41.87	1942
80	80.65	53.42	2759	81.16	51.82	2695	80.93	51.93	2697
90	90.96	63.52	3618	91.76	62.00	3560	91.24	62.07	3558
100	100.7	73.61	4577	101.8	72.19	4529	101.0	72.19	4520
110	109.8	83.64	5630	111.0	82.33	5593	110.1	82.25	5576
120	118.4	93.56	6771	119.7	92.37	6747	118.7	92.20	6720
130	126.5	103.4	7995	128.0	102.3	7987	126.8	102.0	7948
140	134.3	113.0	9300	135.9	112.1	9306	134.5	111.7	9255
150	141.8	122.6	10681	143.5	121.7	10704	142.1	121.2	10637
160	148.7	131.9	12134	150.5	131.2	12175	148.7	130.6	12091
170	154.9	141.1	13652	157.0	140.5	13713	154.9	139.8	13610
180	160.7	150.2	15231	163.0	149.7	15314	160.7	148.8	15189
190	166.1	159.0	16865	168.6	158.6	16972	166.1	157.7	16823
200	171.2	167.6	18552	173.8	167.4	18685	171.2	166.3	18510
210	175.8	176.1	20287	178.4	176.0	20447	176.0	174.8	20245
220	180.2	184.4	22067	182.7	184.4	22252	180.5	183.1	22028
230	184.6	192.5	23892	186.8	192.6	24100	184.9	191.2	23855
240	188.8	200.4	25759	190.6	200.6	25987	189.5	199.2	25726
250	192.8	208.2	27668	194.1	208.5	27911	193.9	207.0	27644
260	196.5	215.9	29614	197.3	216.2	29869	197.9	214.7	29604
270	200.4	223.4	31599	200.5	223.7	31857	201.4	222.2	31601
280	203.6	230.7	33620	203.5	231.0	33877	204.5	229.6	33631
290	206.3	237.9	35670	206.4	238.2	35927	207.1	236.8	35689
298.15	208.3 ± 0.7	243.6 ± 1.5	37360 ± 185	208.7 ± 0.5	244.0 ± 1.2	37619 ± 142	208.8 ± 0.8	242.6 ± 1.5	37384 ± 190
300	208.7	244.9	37746	209.2	245.3	38006	209.2	243.9	37770
310	211.0	251.8	39845	211.8	252.2	40111	210.7	250.8	39870
5	0.134	0.029	0.119	0.137	0.026	0.108	0.143	0.027	0.113

of experimental points from the smoothed curve within a 95-% confidence interval (Fig. 4).

The found thermodynamic functions appreciably increase with increasing europium doping level. The absence of pronounced dependence between the entropy and enthalpy changes and the europium content may be considered as an indicator of that the magnetic interaction between europium atoms, which result in the transitions, occurs as soon as at the lowest concentration, and its further increase does not lead to any essential changes within the studied range of doping.

CONCLUSIONS

Compounds based on barium, tungsten, and REEs, such as lanthanum and europium, have been prepared by solid-phase synthesis. Their structural

and thermodynamic properties have been studied. Based on the X-ray diffraction data, the X-ray diffraction analysis of the samples was performed, and their unit cell parameters and atomic positions have been determined. Heat capacity measurements have been carried out from the liquid helium temperature and, as a result, the low-temperature anomalies related to the magnetic transitions in the structure of the samples due to the presence of doping europium atoms have been found.

FUNDING

This work was performed within project no. AR05130095 within the program of the Science Committee of the Ministry of Education and Science of the Republic of Kazakhstan for financing scientific researches.

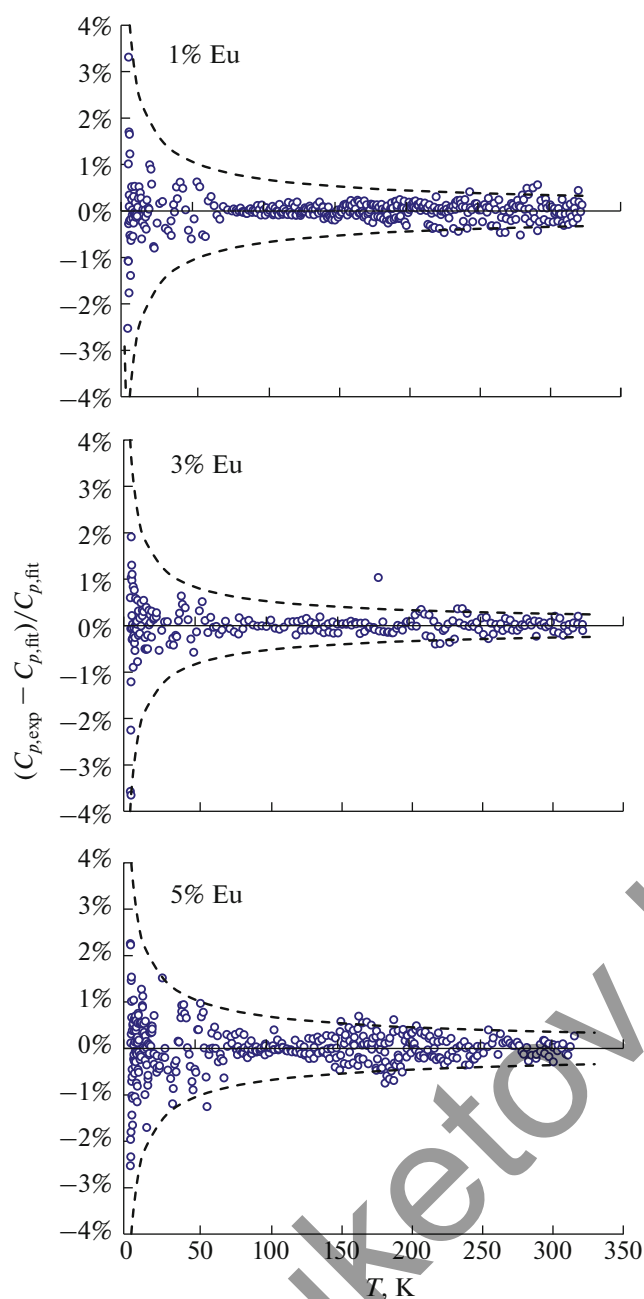


Fig. 4. Spread of experimental heat capacity values from the smoothed curve for the studied $\text{Ba}(\text{La}_{1-x}\text{Eu}_x)_2\text{WO}_7$.

CONFLICT OF INTERESTS

The authors declare that they have no conflict of interests.

REFERENCES

1. I. M. Pinatti, I. C. Nogueir, W. S. Pereira, et al., *Dalton Trans.* **44**, 17673 (2015).
<https://doi.org/10.1039/C5DT01997D>

2. C. Qin, Y. Huang, G. Chen, et al., *Mater. Lett.* **63**, 1162 (2009).
<https://doi.org/10.1016/j.matlet.2009.02.018>
3. G. Braziulis, R. Stankeviciute, and A. Zalga, *Mater. Sci.* **20**, 90 (2014).
<https://doi.org/10.5755/j01.ms.20.1.4797>
4. G. Blasse, G. J. Dirksen, L. H. Brixner, et al., *Mater. Chem. Phys.* **21**, 293 (1989).
<https://doi.org/10.1134/S003602361311017X>
5. S. Choi, B.-Y. Park, H.-K. Jung, et al., *J. Korean Phys. Soc.* **57**, 169 (2010).
<https://doi.org/10.3938/jkps.57.169>
6. S.-A. Yan, J.-W. Wang, Y.-S. Chang, et al., *Opt. Mater.* **34**, 147 (2011).
<https://doi.org/10.1016/j.optmat.2011.07.028>
7. S.-A. Yan, Y.-S. Chang, W.-S. Hwang, et al., *J. Lumin.* **132**, 1867 (2012).
<https://doi.org/10.1016/j.jlumin.2012.02.007>
8. Y. Deng, S. Yi, J. Huang, et al., *Mater. Res. Bull.* **57**, 85 (2014).
<https://doi.org/10.1016/j.materresbull.2014.05.035>
9. S. K. Hussain and J. S. Yu, *Mater. Res. Bull.* **95**, 229 (2017).
<https://doi.org/10.1016/j.materresbull.2017.07.031>
10. T. Matsui, T. Kawase, and K. Naito, *J. Nucl. Mater.* **186**, 254 (1992).
[https://doi.org/10.1016/0022-3115\(92\)90344-K](https://doi.org/10.1016/0022-3115(92)90344-K)
11. E. Bernardo, *J. Non-Cryst. Solids* **354**, 3486 (2008).
<https://doi.org/10.1016/j.jnoncrysol.2008.03.021>
12. J. Faber and T. Fawcett, *Acta Crystallogr. B* **58**, 325 (2002).
<https://doi.org/10.1107/S0108768102003312>
13. J. Rodríguez-Carvajal, *Physica B* **192**, 55 (1993).
[https://doi.org/10.1016/0921-4526\(93\)90108-I](https://doi.org/10.1016/0921-4526(93)90108-I)
14. W. Kraus and G. Nolze, *J. Appl. Crystallogr.* **29**, 301 (1996).
<https://doi.org/10.1107/S0021889895014920>
15. M. R. Bissengaliyeva, D. B. Gogol, Sh. T. Taymasova, et al., *J. Chem. Eng. Data* **56**, 195 (2011).
<https://doi.org/10.1021/je100658y>
16. L. M. Kovba, L. N. Lykova, and V. L. Balashov, *Russ. J. Inorg. Chem.* **30**, 311 (1985).
17. W. T. Fu, D. J. W. Ijdo, and A. Bontenbal, *J. Solid State Chem.* **201**, 128 (2013).
<https://doi.org/10.1016/j.jssc.2013.01.042>
18. A. E. Musikhin, M. A. Bespyatov, V. N. Shlegel, et al., *J. Alloys Compd.* **802**, 235 (2019).
<https://doi.org/10.1016/j.jallcom.2019.06.197>
19. B. H. Justice and E. F. Westrum, Jr., *J. Phys. Chem.* **67**, 339 (1963).
<https://doi.org/10.1021/j100796a031>
20. T. P. Melia and R. Merrifield, *J. Inorg. Nucl. Chem.* **32**, 2573 (1970).
[https://doi.org/10.1016/0022-1902\(70\)80304-9](https://doi.org/10.1016/0022-1902(70)80304-9)
21. M. R. Bissengaliyeva, D. B. Gogol, M. A. Bespyatov, et al., *Mater. Res. Express* **6**, 106109 (2019). 106109.
<https://doi.org/10.1088/2053-1591/ab3ae3>

Translated by E. Glushachenkova